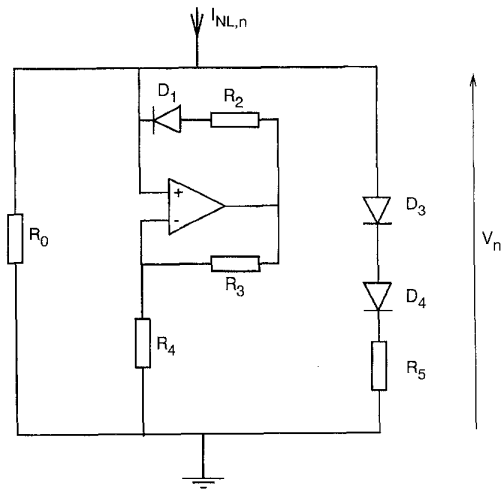
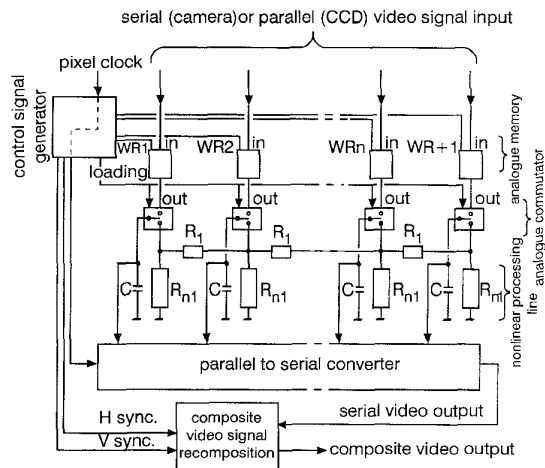


are loaded in the the nonlinear processing line via analogue commutators.



7142

Fig. 2 Nonlinear device, giving current-voltage relation according to eqn. 1



7143

Fig. 3 Acquisition diagram

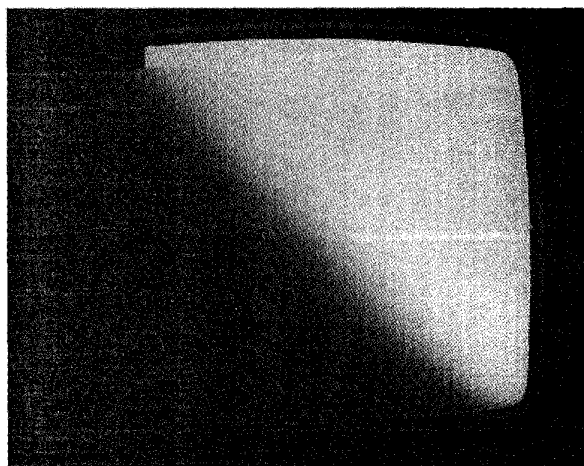


Fig. 4 Front propagation from left to right

Abscissa: cells, $n = 1$ to 48
Ordinate, top to bottom: time, such as the whole height corresponds to 20ms

To check the experimental setup, we compare a real front propagation and the theoretical prediction. The capacity in parallel is 33nF, while the resistors have been chosen so that $R_0 = 17k\Omega$ and $R_1 = 680\Omega$. In this case, $d = 25$ and the continuity criterion is verified. The nonlinear parameters V_a and V_b of all the cells are fixed at $V_a = 0.68V$ and $V_b = 1.23V$. Then, as $2V_a > V_b$, only the steady state $V_n = 0V$ can propagate (that is with + in eqns. 6 and 7). To observe the propagation of this steady state, the initial condition loaded in the lattice consists in setting all the cells to $V = V_b$, except the five first cells on the left, which are set to $V_n = 0V$ ($n = 1 - 5$) to take into account the Neumann boundary conditions. Fig. 4 shows a rapid adaptation of the initial conditions to a front profile, followed by propagation of the steady state $V_n = 0V$ from left to right.

Using an oscilloscope to quantify the velocity of the front, we obtain $c_{exp} = 2125\text{cell/s}$, which is in good agreement with the theoretical value $c = 2240\text{cell/s}$, calculated with eqn. 7.

Conclusions: We have presented an experimental device which allows us to study Nagumo's equation. Our first result shows a good agreement between theoretical and experimental results. As the discretisation parameter d can be easily changed by changing the coupling resistor, it will be interesting to observe, in a later study, the discretisation effects on propagation.

© IEE 1998

3 April 1998

Electronics Letters Online No: 19980774

S. Binczak, J.C. Comte, B. Michaux, P. Marquié and J.M. Bilbault (University of Burgundy, LE21, 21000 Dijon, France)

E-mail: stbinc@u-bourgogne.fr

References

- SCOTT, A.C.: 'The electrophysics of a nerve fiber', *Rev. Mod. Phys.*, 1975, **47**, pp. 487-534
- MURRAY, J.D.: 'Mathematical biology' (Springer-Verlag, Berlin, 1989)
- MARQUIÉ, P., BINCAZAK, S., COMTE, J.C., MICHAUX, B., and BILBAULT, J.M.: 'Diffusion effects in a nonlinear diffusive lattice', to be published in *Phys. Rev. E*, May 1998
- NAGUMO, J., ARIMOTO, S., and YOSHIZAWA, S.: 'An active pulse transmission line simulating nerve axon', *Proc. IRE*, 1962, **50**, pp. 2061-2070
- ANDERSON, A.R.A., and SLEEMAN, B.D.: 'Wave front propagation and its failure in coupled systems of discrete bistable cells modelled by FitzHugh-Nagumo dynamics', *Int. J. Bifurcation Chaos*, 1995, **5**, (1), pp. 63-74
- LAPLANTE, J.P., and ERNEUX, T.: 'Propagation failure in arrays of coupled bistable chemical reactors', *Phys. Chem. J.*, 1992, **96**, pp. 4931-4934
- KEENER, J.P.: 'Propagation and its failure in coupled systems of discrete excitable cells', *SIAM J. Appl. Math.*, 1987, **3**, pp. 556-572
- ERNEUX, T., and NICOLIS, G.: 'Propagating waves in discrete bistable reaction-diffusion systems', *Physica D*, 1993, **67**, pp. 237-244

High resolution wideband direction finding arrays based on optimum symmetrical number system encoding

D.C. Jenn, P.E. Pace, T. Hatzithanasiou and R. Vitale

A new interferometer direction finding (DF) array architecture based on the optimum symmetrical number system (OSNS) is presented. OSNS arrays are capable of unambiguous high resolution DF over a wide bandwidth and field of view with as few as three elements, with multiple baseline options. A three-element array was designed, fabricated and tested at 8.5GHz to verify the OSNS concepts experimentally.

Introduction: Symmetrical number systems have been used previously to increase the efficiency of folding analogue-to-digital converter architectures, efficiently encode digital antenna links, and increase the resolvable bandwidth of two- and three-channel digital intercept receivers [1 - 4]. Another application where folded

waveforms occur is phase interferometry for direction finding (DF). The phase sampled linear interferometer is a well-known DF approach [5 – 7] using the known spacing between two or more array elements to obtain time-of-arrival relationships. Time-of-arrival measurements can be converted into phase differences which are then used to determine the angle of arrival (AOA).

Multiple baseline systems generally consist of a reference antenna in the centre of two or more other antennas spaced at different distances from it. Widely spaced elements are required for high-resolution AOA estimates, but are also highly ambiguous. Ambiguities which arise from arrays with long baselines (element spacings) are generally resolved by using another more closely spaced baseline pair with no ambiguities. In principle, sufficient information is available from three elements to uniquely determine the AOA of a single emitter without limitation on the minimum element spacing.

This Letter describes the development of a new type of phase-sampled DF array based on the optimum symmetrical number system (OSNS) [1]. The OSNS DF antenna architecture being investigated uses the OSNS to decompose the analogue spatial filtering operation into a number of parallel sub-operations (moduli) that are of smaller complexity. One two-element interferometer is used for each sub-operation and only requires precision in accordance with its modulus. A much higher spatial resolution is achieved after the spatial filtering results from the individual low-resolution arrays are recombined. There are no theoretical limits on the array baseline or unambiguous AOA resolution. In the absence of noise and system errors, the minimum element spacing and AOA resolution are limited by the physical size of the array radiating elements and the complexity of the decoding electronics (i.e. the number of comparators required).

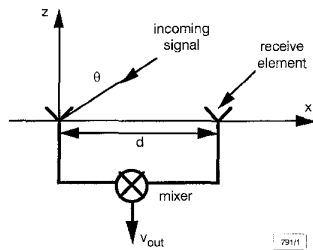


Fig. 1 Two-element phase interferometer

OSNS direction finding antenna design: A two-element interferometer array is shown in Fig. 1. The relationship between the angle of incidence of the plane wave (θ) and the phase difference between the signals from the two elements is

$$\Delta\phi = (2\pi d/\lambda) \sin\theta + \psi_0 \quad (1)$$

where λ is the wavelength, d is the element spacing, and ψ_0 accounts for any transmission line phase differences between the two elements. The element outputs are combined in a mixer. Since the two signals are at the same frequency, the mixer output voltage is only a function of the AOA:

$$v_{out} = \frac{A^2}{2} \cos\left(\frac{2\pi d}{\lambda} \sin\theta + \psi_0\right) \quad (2)$$

where A is the magnitude of the voltage from the elements owing to plane wave excitation. The mixer output voltage is a symmetrical folding waveform (a sinusoid), and the number of folds n that occur when an emitter is swept from $-90^\circ \leq \theta \leq 90^\circ$ increases with distance between the elements as

$$n = (2d)/\lambda \quad (3)$$

A symmetrically folded waveform can be represented by an optimum SNS of modulus m with integer values given by the row vector

$$[0, 1, \dots, m-1, m-1, \dots, 1, 0]$$

such that the period of the waveform is twice the modulus.

When more than one fold (period) is present, there is an ambiguity; a single voltage corresponds to several possible AOAs. Such ambiguities can be resolved by using additional arrays such that all the moduli are, pairwise, relatively prime with each other. If N channels (pairs of elements) are used, the number of spatial quantisation cells (dynamic range) is

$$M = \prod_{i=1}^N m_i \quad (4)$$

All of the channels can share a common element. Therefore, an N channel array requires $N + 1$ elements. The required spacing between the reference element and the second element of channel i is

$$d_i = (n_i\lambda)/4 = (M\lambda)/(4m_i) \quad (5)$$

The spatial resolution near boresight is given by

$$r = FOV/M \quad (6)$$

where FOV is the field of view determined by the receiving element pattern. Ideally, the FOV can be 180° . The spatial resolution decreases with the angle off of boresight, because of the $\sin\theta$ dependence in eqn. 2.

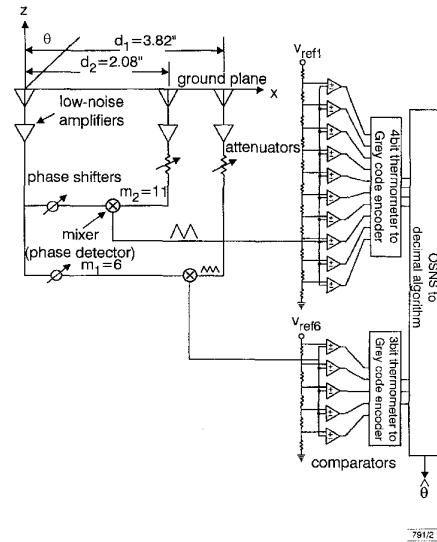


Fig. 2 Block diagram of OSNS array based on moduli $m_1 = 6$ and $m_2 = 11$

A two-channel OSNS array is shown in Fig. 2. An array based on the moduli $m_1 = 6$ and $m_2 = 11$ was designed, fabricated and tested at 8.5GHz. The radiating elements are open-ended waveguides. To provide an adequate signal-to-noise ratio, a low-noise amplifier is included at the output of each interferometer element. Since the common element splits the signal into N paths, an attenuator is placed in the other branches to balance the amplitudes. The amplifiers operate in saturation so that the mixer input signal levels are independent of the angle of incidence. A fixed phase shifter is also included in one branch of each interferometer so that the symmetrically folded phase response waveforms from each mixer may be aligned. This alignment insures that the comparators in the digital processor properly sample the phase waveform and encode it in the OSNS. The measured mixer outputs are shown in Fig. 3.

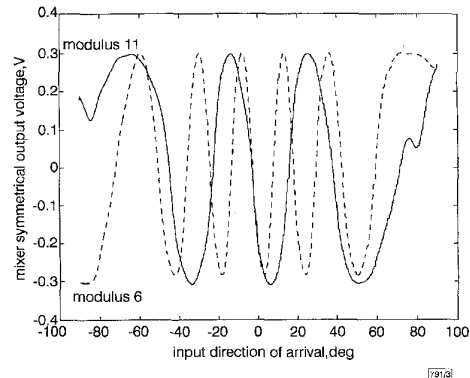


Fig. 3 Measured mixer output voltage for three-element OSNS array

The number of comparators required for a channel with modulus m_i is $m_i - 1$. Thus, the total number of comparators for the array shown in Fig. 2 is $\sum_{i=1}^N (m_i - 1) = 15$. The measured transfer function, when decoded to give the AOA, gives the plot shown in Fig. 4. The spikes are due to errors and imperfections in the transmission line phases and comparator settings, which lead to encoding errors. These errors can, however, be isolated and interpolation schemes used to correctly resolve the AOA [8].

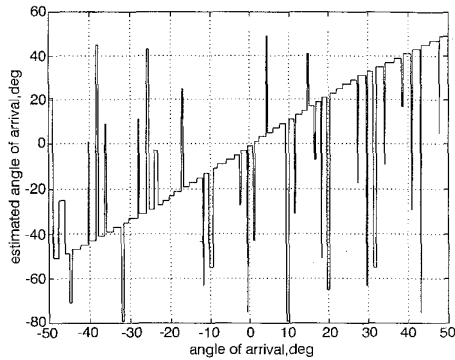


Fig. 4 Measured transfer function of three-element OSNS array based on $m_1 = 6$ and $m_2 = 11$

Summary and conclusions: A new phase sampling direction finding architecture based on the optimum symmetrical number system has been presented. Eqns. 4 and 6 describe the tradeoffs involved in the design of an OSNS array. The spatial resolution, that is, the angular resolution of the direction measurement, is determined by M . The resolution is B , typically expressed in bits. Thus, the equivalent number of bits resolution is obtained from $M = 2^B$

According to eqn. 4, M can be increased by increasing either the number of moduli, or the values of the individual moduli. Since each m_i in eqn. 4 is equivalent to a channel, to increase M without adding elements requires an increase in the values of m_i . The spacing of the elements is specified in eqn. 5. In general, as m_i decreases, the channel spacing decreases but the number of comparators increases.

Table 1: Several OSNS arrays that have same spatial resolution

OSNS moduli	Element spacings	Comparators required
$m_1=3, m_2=20$	$d_1=5\lambda, d_2=0.75\lambda$	21
$m_1=4, m_2=15$	$d_1=3.75\lambda, d_2=1\lambda$	17
$m_1=5, m_2=12$	$d_1=3\lambda, d_2=1.25\lambda$	15
$m_1=3, m_2=4, m_3=5$	$d_1=5\lambda, d_2=3.75\lambda, d_3=3\lambda$	9

There are three major advantages of the OSNS DF architecture. First, it has a wide instantaneous field of view that is only limited by the receiving element pattern edge effects. The DF process does not require any antenna steering or beam scanning. This is critical for intercepting low probability of intercept signals. Secondly, the architecture is capable of wideband operation. The transmission lines incorporated in the feed do not have to compensate for space delays as they do in many scanning arrays. Therefore the line lengths can be kept short. Finally, the OSNS architecture has the ability to provide high resolution DF with as few as three closely spaced elements, which can be arranged in a number of possible configurations. For example, Table 1 contains the spacings for four different OSNS arrays that have the same spatial resolution ($M = 60$). In some applications, element placement at certain locations on the platform may be prohibited, in which case an alternate OSNS design could be used to provide the same unambiguous AOA resolution.

© IEE 1998

2 April 1998

Electronics Letters Online No: 19980811

D.C. Jenn, P.E. Pace, T. Hatzithanasiou and R. Vitale (Center for Joint Services Electronic Warfare, Naval Postgraduate School, Monterey, CA 93943, USA)

References

- 1 PACE, P., SCHAFER, J., and STYER, D.: 'Optimum analog preprocessing for folding ADCs', *IEEE Trans. Circuits Syst. II: Analog Digit. Signal Process.*, 1995, **42**, pp. 825-829
- 2 PACE, P., RAMAMOORTHY, P., and STYER, D.: 'A preprocessing architecture for resolution enhancement in high-speed analog-to-digital converters', *IEEE Trans. Circuits Syst. II: Analog Digit. Signal Process.*, 1994, **41**, pp. 373-379
- 3 PACE, P., RINGER, W., FOSTER, K., and POWERS, J.: 'Optical signal integrity and interpolation signal processing in wideband SNS digital antennas'. Proc. 1997 DARPA Photonic Systems for Antenna Applications, 13 January 1997.
- 4 PACE, P., LEINO, R., and STYER, D.: 'Use of the symmetrical number system in resolving single-frequency undersampling aliases', *IEEE Trans. Signal Process.*, 1997, **SP-45**, pp. 1153-1160
- 5 LIPSKY, S.: 'Microwave passive direction finding' (Wiley, 1987)
- 6 JOHNSON, R., and MINER, G.: 'Algorithms for radio direction finding', *IEEE Trans. Aerosp. Electron. Syst.*, 1986, **AES-22**, (4), pp. 432
- 7 JACOBS, E., and RALSTON, E.: 'Ambiguity resolution in interferometry', *IEEE Trans. Aerosp. Electron. Syst.*, 1981, **AES-17**, (6), pp. 766-780
- 8 NAUTA, B., and VENES, A.G.W.: 'A 70MS/s 1 10-mW 8-b CMOS folding and interpolating A/D converter', *IEEE J. Solid-State Circuits*, 1995, **SSC-30**, pp. 1302-1308

Improved channel estimation with decision feedback for OFDM systems

M. Bossert, A. Donder and V. Zyablov

An improved channel estimation strategy for a continuous orthogonal frequency division multiplexing transmission scheme is presented, based on feedback from decoding decisions of forward error correction of the information data. No special redundancy, such as pilot tones, is required.

Introduction: For coherent transmission of information in orthogonal frequency division multiplexing (OFDM) systems, it is necessary to compensate the amplitude and phase distortions which are introduced by the channel. Usually, a set of pilot tones is used from which the channel transfer function can be interpolated at the receiver, which in turn reduces the effective data rate. In [1], a method is proposed which uses received data decisions combined with a noise reduction strategy to track the channel transfer function and thus needs no special redundancy, such as pilot tones, as long as a continuous transmission of OFDM symbols is considered. This method is investigated in detail in [2], combined with forward error correction which reduces the influence of decision errors. After estimating the transfer function of a received symbol, this estimate is used for the demodulation of the next symbol. As long as the channel is varying slowly, this method works well, but in the case of mobile radio channels, the estimation may give a residual error due to the variation of the channel from one symbol to another. To overcome this effect, we propose to predict the latest transfer function for demodulation through the use of previous transfer functions.

Brief system description: We consider an OFDM system of N subchannels, each having a bandwidth of F . Thus, the overall bandwidth is $F_{tot} = NF$. In each OFDM symbol a vector $\mathbf{S} = (S_0, \dots, S_{N-1})$ will be transmitted with S_i being a symbol from a complex valued alphabet. The corresponding time domain vector $\mathbf{s} = (s_0, \dots, s_{N-1})$ is obtained by applying the IFFT on \mathbf{S} , i.e. $\mathbf{s} = \text{IFFT}\{\mathbf{S}\}$. This vector corresponds to a series of time samples, spaced by $T = 1/NF$. Before transmitting the signal, a cyclic extension by $L - 1$ samples of the time vector is performed, i.e. we form $\mathbf{s}_{ext} = (s_{N-L}, \dots, s_{N-1}, \mathbf{s})$. The cyclic extension must guarantee that $LT \geq \tau_{max,hs}$, i.e. it has to be greater than the channel impulse response. For further details, see [1]. If this condition is fulfilled, it can be shown that received values $U_i^{(k)}$ of the individual subchannels of the k th OFDM symbol can be written as

$$U_i^{(k)} = S_i^{(k)} \cdot H_i^{(k)} + N_i^{(k)} \quad i = 0, \dots, N - 1$$